Progress In Electromagnetics Research M, Vol. 41, 149–158, 2015

A Semi-Analytical Method to Calculate the Entries of the Method of Moments Matrix for the Mixed Potential Integral Equation of a Source Reconstruction Problem

Saffet Gokcen Sen*

Abstract—In this article, the mixed potential integral equation is discretized using the Rao-Wilton-Glisson basis functions in order to obtain a method of moments matrix equation for a source reconstruction problem. The weighting functions used in the setup of the moments equation are Dirac delta functions. The entries of the moments matrix are computed using a semi-analytical method which is applicable to any method of moments problem with point matching. The analytical calculation is made possible by employing a differentiation property of the scalar Green function and the properties of the mesh elements of the source plane. The semi-analytical method makes it easier to increase the accuracy of the moments matrix elements. The accuracy of the method is shown by comparing the results obtained using the semi-analytical method to those obtained by a fully numerical procedure.

1. INTRODUCTION

The source reconstruction for a specific electromagnetic field distribution is the procedure of either setting up equivalent electromagnetic problems in order to determine equivalent sources or determining the actual sources by solving the related integral equations. The source reconstruction method is used in several areas which can be mentioned as near-field to far-field (NF-FF) transformation, microwave imaging, antenna design, antenna characterization, antenna diagnostics, electromagnetic interference estimation in electronic circuits, corrections in antenna measurements, radome defect localization. The most important aspect of the source reconstruction method is that it takes the electromagnetic problem into consideration just as it is, with all of the real world factors included through the electromagnetic field measurement results.

The literature on the source reconstruction method can be divided into two parts with respect to the type of the integral equation formulation for the problem. In the first group, a single integral equation formulation is done whereas in the second group, a dual-integral equation formulation is preferred. In the single equation formulation, the equivalent sources obtained using the equivalence principle are related to the field measurement results using the radiation integrals. In the dual equation formulation, an extra equation is set up using the Love's equivalence principle at the measurement surface. Some of the articles in the single equation formulation group are to be cited now. In [7–30], several NF-FF transformation formulations using the source reconstruction method and the related applications are studied. In [7], equivalent magnetic currents are constructed on a plane including the aperture of an antenna using the near electric field data on a plane. These currents are then used to calculate the far-field. In [8], equivalent magnetic currents are built on a plane including the aperture of an antenna again. However, the near electric field data is not necessarily to be obtained on a plane and can be gotten from a surface with an arbitrary geometry. In [9], an equivalent electric current is set up on a

Received 26 January 2015, Accepted 2 March 2015, Scheduled 8 March 2015
* Corresponding author: Saffet Gokcen Sen (saffetgokcensen@hotmail.com).
The author is with the Electrical Engineering Department, Ataturk University, Turkey.

plane including the aperture of an antenna using the near electric field data obtained on an arbitrary surface. It is also indicated that the near field data need not satisfy the Nyquist sampling criteria. In [10], equivalent magnetic currents are reconstructed on a plane enclosing the antenna by using the near electric field data on a circle. [11] is about the reconstruction of an equivalent magnetic current on an arbitrary surface enclosing the antenna. The reconstruction is carried out by means of amplitude-only electric field data acquired over arbitrary surfaces. In [12], equivalent magnetic currents are constructed over a plane enclosing the antenna using the near electric field data obtained by spherical scanning. A special strategy which is based on first neglecting the radial field component and then the retrieval of it through an iterative algorithm is used in the reconstruction process. In [13], the near electric field data of the radiating structure is used to construct equivalent electric and magnetic currents tangential to an arbitrary 3-D surface. [14] reports an application of the sources reconstruction method to the near-field antenna measurements. The antenna-pattern of the probe used in the near-field antenna measurements is taken into account to eliminate the probe distortion to the measurements. [15] is about enhancing the analysis of printed reflectarrays in the Fresnel zone of the primary feed which is a horn antenna. The enhancement is achieved by means of the source reconstruction method which transforms the measured far field of the horn to its near field to calculate the field on the reflectarray. In [16], the source reconstruction method which uses electric field data to construct equivalent electric and magnetic currents is accelerated by the multilevel fast multipole method. The source reconstruction method mentioned in [17] is stated to have the capability of resolving equivalent currents smaller than half a wave length which means that this method goes beyond the sampling limitation set by the Nyquist sampling criterion. In [18], the interaction of a radome with a reflector antenna covered by the radome is examined using the source reconstruction method. The equivalent electric and magnetic currents are constructed on the radome surface using the near electric field data. The reconstructed currents exhibit the defects in the radome. In [19], the source reconstruction method is used to determine the geometry of metallic bodies on a 2-D domain. [20] is related with using the source reconstruction method for the accurate modeling of the noise sources in an electronic circuit and the estimation of the noise to be radiated by the circuit. [21] is about employing the graphical processing unit(GPU) with the memory saving technique to calculate the elements of the impedance matrix of the integral equation to find the equivalent currents. [22] describes the use of the source reconstruction method for the modeling of a frequency scanning antenna array of an imaging system. In [23], a source reconstruction algorithm which is different from the conventional source reconstruction algorithms working at a single frequency is developed for structures radiating over a wide frequency band. The proposed algorithm is stated to have a low computational cost. In [24], an iterative source reconstruction method which uses amplitude only near electric field data is proposed. This method is shown to have the capability of reproducing the original radiation pattern accurately in every direction. [25] explains a new accelerator scheme for the source reconstruction method to determine the metallic parts of the structure under test by using more than one GPU's. In the following references, the dual-integral equation formulation is used. In [26], the dual-integral formulation is employed to construct equivalent electric and magnetic currents on arbitrary 3-D surfaces. In order to check the accuracy of the method, the reconstructed currents and the original currents are compared in addition to the comparison of the reconstructed fields to the original fields. The method is stated to be very appropriate for the diagnostic tasks due to its high accuracy in reconstructing the original currents. In [27], several integral formulations for the source reconstruction are compared to each other. The dual-integral equation formulation is demonstrated to provide robust field reconstruction in the close vicinity of actual radiators for a wide range of signal to noise ratio in the measured field data. In [28], different formulations of the source reconstruction problem on an arbitrary 3-D closed surface are examined in detail. The dual-integral formulation is derived using the Love's equivalence principle. The stability and usefulness of this formulation is demonstrated. [29] reports the use of the dual-integral equation formulation in the post-processing of antenna measurements to correct the radiation pattern of the antenna under test to the extent as if it had been measured in an ideal environment. [30] is about the integration of the fast multipole method to the dual-integral equation formulation for the application of the source reconstruction to electrically large scatterers.

In this article, using the mixed potential integral equation formulation, an x-directed point source is to be reconstructed using its electric field data. The source reconstruction surface is a square containing

the actual source. The electric field data is on a hemisphere the center of which is the center of the source reconstruction plane. The unknown current is expanded in terms of the Rao-Wilton-Glisson (RWG) basis functions. The reconstruction plane is discretized using triangular meshing. The discretized form of the reconstruction problem is actually a method of moments matrix equation. The calculation of the entries of the moments matrix involves the calculation of some integrals containing the scalar Green's function. For this calculation, a simple semi-analytical method is proposed and shown to work well by comparing the method results to those of a fully numerical procedure. The advantage of this method to the others in the literature is that it employs analytical evaluation of half of some double integrals which contribute to the entries of the moments matrix. Due to this analytical evaluation, it is easier to increase the accuracy of the moments matrix elements in this method compared to a fully numerical procedure. In the two dimensional integrals half of which can be calculated analytically, a one dimensional quadrature is needed to calculate the whole integral. In order to increase the accuracy of the quadrature, its order must be increased. It is always easier to build one dimensional high order quadratures than building high order two dimensional quadratures. Hence, the advantage and contribution of the semi-analytical method is that it is easier to increase the accuracy of the moments matrix elements using the semi-analytical method. In the Section 2, the reconstruction problem is formulated and its solution is explained. The semi-analytical method is described. In the Section 3, the semi-analytical method is shown to work well by comparing the method results to those of a fully-numerical procedure.

2. THE DESCRIPTION AND SOLUTION OF THE PROBLEM

A point source denoted by

$$\vec{J}(x,y,z) = \hat{x}\ Il\ \delta(x)\,\delta(y)\,\delta(z) \tag{1}$$

with

$$Il = 1A \cdot m \tag{2}$$

resides at the origin of the spherical coordinate system. The θ and ϕ components of the electrical field formed by this source are sampled on the surface of a hemisphere centered at the origin. Assuming a time harmonic dependence of $e^{-j\omega t}$ with j being the imaginary unit, ω being the angular frequency and t being time, this electric field can be written by using the equation:

$$\vec{E} = j\omega\vec{A} - \vec{\nabla}\phi \tag{3}$$

where $\vec{A}$ is the vector magnetic potential and ϕ is the scalar potential. The point source is to be reconstructed using the electric field samples. That is the mean, the weighting function in the construction of the method of moments matrix is the Dirac delta function. The mixed potential integral equation to be discretized is as follows:

$$E_i(\vec{r}) = \frac{j\omega\mu}{4\pi}\int_S J_i(\vec{r}\,')\frac{e^{jk|\vec{r}-\vec{r}\,'|}}{|\vec{r}-\vec{r}\,'|}ds' - \frac{1}{j\omega 4\pi\epsilon}\frac{\partial}{\partial i}\int_S \vec{\nabla}'_s\cdot\vec{J}(\vec{r}\,')\frac{e^{jk|\vec{r}-\vec{r}\,'|}}{|\vec{r}-\vec{r}\,'|}ds' \quad (i=x,y,z) \tag{4}$$

In (4), μ and ϵ are the permeability and the permittivity of the medium respectively. S is the source reconstruction plane. $\vec{r}$ is the position vector of the field point given by

$$\vec{r} = \hat{x}x + \hat{y}y + \hat{z}z \tag{5}$$

and $\vec{r}\,'$ is the position vector of the source coordinates given by

$$\vec{r}\,' = \hat{x}x' + \hat{y}y' + \hat{z}z' \tag{6}$$

The source reconstruction plane is the x-z plane. Hence, the differential area element denoted by ds' is given as

$$ds' = dx'dz' \tag{7}$$

The electric current density is expanded in terms of RWG basis functions to obtain

$$\vec{J}(\vec{r}\,') = \sum_{n=1}^{N} I_n\vec{f}_n(\vec{r}\,') \tag{8}$$

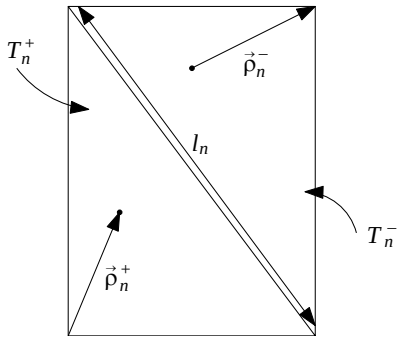

Figure 1. A typical triangle pair in the mesh structure of the source reconstruction plane.

In (8), $\vec{f}_n(\vec{r}\,')$ are RWG basis functions and I_n are the expansion coefficients. The source reconstruction plane is meshed into triangles which are known to be the same as the ones shown in Fig. 1. This typical triangle pair is used to make the definitions related with the RWG basis functions.

The RWG basis function $\vec{f}_n(\vec{r})$ is defined as follows:

$$\vec{f}_n(\vec{r}) = \begin{cases} \dfrac{l_n}{2A_n^+}\vec{\rho}_n^+ & \text{if } \vec{r} \text{ in } T_n^+ \\ \dfrac{l_n}{2A_n^-}\vec{\rho}_n^- & \text{if } \vec{r} \text{ in } T_n^- \\ 0 & \text{if otherwise} \end{cases} \tag{9}$$

where T_n^+ is the triangle on the left and T_n^- is the triangle on the right in Fig. 1. $\vec{\rho}_n^+$ is the vector drawn from the free vertex of T_n^+ to a point with the position vector $\vec{r}$ in T_n^+. $\vec{\rho}_n^-$ is the vector drawn from a point with the position vector $\vec{r}$ in T_n^- to the free vertex of T_n^-. A_n^+ is the area of the triangle T_n^+. A_n^- is the area of the triangle T_n^-. l_n is the length of the side common to the triangles. A property of the RWG basis functions related with surface divergence is given in [1] as follows:

$$\vec{\nabla}_s \cdot \vec{f}_n(\vec{r}) = \begin{cases} \dfrac{l_n}{A_n^+} & \text{if } \vec{r} \text{ in } T_n^+ \\ -\dfrac{l_n}{A_n^-} & \text{if } \vec{r} \text{ in } T_n^- \\ 0 & \text{if otherwise} \end{cases} \tag{10}$$

If the expansion in (8) is used in (4) along with the property given in (10), then the following discretized integral equation is reached:

$$\begin{aligned} E_i(\vec{r}) = \sum_{n=1}^{N} & \frac{j\omega\mu}{4\pi}\int_{T_n^+} I_n \frac{l_n}{2A_n^+}\left(\vec{\rho}_n^+\right)_i \frac{e^{jk|\vec{r}-\vec{r}\,'|}}{|\vec{r}-\vec{r}\,'|}ds' + \frac{j\omega\mu}{4\pi}\int_{T_n^-} I_n \frac{l_n}{2A_n^-}\left(\vec{\rho}_n^-\right)_i \frac{e^{jk|\vec{r}-\vec{r}\,'|}}{|\vec{r}-\vec{r}\,'|}ds' \\ & -\frac{1}{j\omega 4\pi\epsilon}\int_{T_n^+} I_n \frac{l_n}{A_n^+}\frac{\partial}{\partial i}\left(\frac{e^{jk|\vec{r}-\vec{r}\,'|}}{|\vec{r}-\vec{r}\,'|}\right)ds' + \frac{1}{j\omega 4\pi\epsilon}\int_{T_n^-} I_n \frac{l_n}{A_n^-}\frac{\partial}{\partial i}\left(\frac{e^{jk|\vec{r}-\vec{r}\,'|}}{|\vec{r}-\vec{r}\,'|}\right)ds' \quad (i = x, y, z) \end{aligned} \tag{11}$$

Using this discretized integral equation, the following method of moments matrix equation is obtained:

$$\begin{bmatrix} \mathbf{E}_{\boldsymbol{\theta}} \\ \mathbf{E}_{\boldsymbol{\phi}} \end{bmatrix} \mathbf{I} = \begin{bmatrix} \mathbf{b}_{\boldsymbol{\theta}} \\ \mathbf{b}_{\boldsymbol{\phi}} \end{bmatrix} \tag{12}$$

$\mathbf{E}_{\boldsymbol{\theta}}$ and $\mathbf{E}_{\boldsymbol{\phi}}$ are both $M \times N$ matrices where M is the number of sampling points on the hemisphere and N is the number of RWG basis functions. $\mathbf{E}_{\boldsymbol{\theta}(p,q)}$ and $\mathbf{E}_{\boldsymbol{\phi}(p,q)}$ denote the elements in the row p, column q of the matrices $\mathbf{E}_{\boldsymbol{\theta}}$ and $\mathbf{E}_{\boldsymbol{\phi}}$ respectively and are given by

$$\mathbf{E}_{\boldsymbol{\theta}}(\mathbf{p}, \mathbf{q}) = I_x^{p,q}\cos(\theta_p)\cos(\phi_p) + I_y^{p,q}\cos(\theta_p)\sin(\phi_p) - I_z^{p,q}\sin(\theta_p) \tag{13}$$

$$\mathbf{E}_{\boldsymbol{\phi}}(\mathbf{p}, \mathbf{q}) = -I_x^{p,q}\sin(\phi_p) + I_y^{p,q}\cos(\phi_p) \tag{14}$$

θ_p and ϕ_p are the θ and ϕ coordinates of the pth sampling point. The integrals I_i^{pq} $(i = x, y, z)$ are defined as

$$I_i^{pq} = \frac{j\omega\mu}{4\pi}\int_{T_{n_q}^+}\frac{l_{n_q}}{2A_{n_q}^+}\left(\vec{\rho}_{n_q}^+\right)_i\frac{e^{jk|\vec{r}_p-\vec{r}_q'|}}{|\vec{r}_p-\vec{r}_q'|}ds' + \frac{j\omega\mu}{4\pi}\int_{T_{n_q}^-}\frac{l_{n_q}}{2A_{n_q}^-}\left(\vec{\rho}_{n_q}^-\right)_i\frac{e^{jk|\vec{r}_p-\vec{r}_q'|}}{|\vec{r}_p-\vec{r}_q'|}ds'$$
$$-\frac{1}{j\omega 4\pi\epsilon}\int_{T_{n_q}^+}\frac{l_{n_q}}{A_{n_q}^+}\frac{\partial}{\partial i}\left(\frac{e^{jk|\vec{r}_p-\vec{r}_q'|}}{|\vec{r}_p-\vec{r}_q'|}\right)ds' + \frac{1}{j\omega 4\pi\epsilon}\int_{T_{n_q}^-}\frac{l_{n_q}}{A_{n_q}^-}\frac{\partial}{\partial i}\left(\frac{e^{jk|\vec{r}_p-\vec{r}_q'|}}{|\vec{r}_p-\vec{r}_q'|}\right)ds' \quad (i = x, y, z) \quad (15)$$

The quantities $T_{n_q}^+$, $T_{n_q}^-$, $A_{n_q}^+$, $A_{n_q}^-$, $\vec{\rho}_{n_q}^+$, $\vec{\rho}_{n_q}^-$ and l_{n_q} are related with the qth RWG basis function. $\vec{r}_q'$ is the position vector of a point in the triangle pair of the qth RWG basis function. $\vec{r}_p$ is the position vector of the pth sampling point. The column vector $\mathbf{I}$ in (12) is an $N \times 1$ matrix and $\mathbf{I}(q, 1)$ is the coefficient I_q used in (8). $\mathbf{b}_{\boldsymbol{\theta}}$ and $\mathbf{b}_{\boldsymbol{\phi}}$ are both $M \times 1$ matrices. $\mathbf{b}_{\boldsymbol{\theta}}(p, 1)$ and $\mathbf{b}_{\boldsymbol{\phi}}(p, 1)$ are the θ and ϕ components of the electric field respectively at the pth sampling point. In order to solve the matrix equation, I_i^{pq} defined in (15) must be calculated. The last two integrals in (15) are calculated in a semi-analytical fashion which is the subject matter of this article. The analytical evaluation is enabled by using the following property:

$$\frac{\partial}{\partial i}\left(\frac{e^{jk|\vec{r}_p-\vec{r}_q'|}}{|\vec{r}_p-\vec{r}_q'|}\right) = -\frac{\partial}{\partial i'}\left(\frac{e^{jk|\vec{r}_p-\vec{r}_q'|}}{|\vec{r}_p-\vec{r}_q'|}\right) \quad (i = x, y, z) \quad (16)$$

It is known that there are only two types of triangles in the mesh of the source reconstruction plane. The first type is shown in Fig. 2(a). Referring to this triangle, the analytical evaluation for the integral with the $\frac{\partial}{\partial x'}$ operator is carried out as follows:

$$\int_{T_{n_q}}\frac{l_{n_q}}{A_{n_q}}\frac{\partial}{\partial x'}\left(\frac{e^{jk|\vec{r}_p-\vec{r}_q'|}}{|\vec{r}_p-\vec{r}_q'|}\right)ds' = \int_{z_1'}^{z_2'}\int_{f_1(z')}^{f_2(z')}\frac{l_{n_q}}{A_{n_q}}(-1)\frac{\partial}{\partial x'}\left(\frac{e^{jk|\vec{r}_p-\vec{r}_q'|}}{|\vec{r}_p-\vec{r}_q'|}\right)dx'dz'$$
$$= \int_{z_1'}^{z_2'}\frac{l_{n_q}}{A_{n_q}}(-1)\left[\left(\frac{e^{jk|\vec{r}_p-\vec{r}_q'|}}{|\vec{r}_p-\vec{r}_q'|}\right)_{x'\to f_2(z')} - \left(\frac{e^{jk|\vec{r}_p-\vec{r}_q'|}}{|\vec{r}_p-\vec{r}_q'|}\right)_{x'\to f_1(z')}\right]dz' \quad (17)$$

Now, the two dimensional integral is reduced to a one dimensional integral. In (17), $f_1(z')$ and $f_2(z')$ are defined as follows:

$$f_1(z') = x_1' = x_2' \quad (18)$$
$$f_2(z') = x_2' + \left(\frac{x_2'-x_3'}{z_2'-z_3'}\right)(z'-z_2') \quad (19)$$

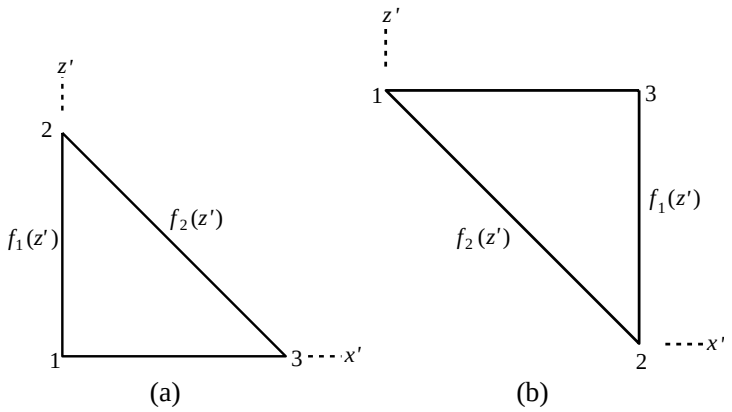

Figure 2. The triangle types in the mesh of the source reconstruction plane. (a) The first triangle type. (b) The second triangle type.

For the same triangle, the analytical evaluation for the integral with the $\frac{\partial}{\partial z'}$ operator is carried out as follows:

$$\int_{T_{n_q}} \frac{l_{n_q}}{A_{n_q}} \frac{\partial}{\partial z'} \left(\frac{e^{jk|\vec{r}_p - \vec{r}'_q|}}{|\vec{r}_p - \vec{r}'_q|} \right) ds' = \int_{x'_1}^{x'_3} \int_{f_2(x')}^{f_1(x')} \frac{l_{n_q}}{A_{n_q}} (-1) \frac{\partial}{\partial z'} \left(\frac{e^{jk|\vec{r}_p - \vec{r}'_q|}}{|\vec{r}_p - \vec{r}'_q|} \right) dz' dx'$$

$$= \int_{x'_1}^{x'_3} \frac{l_{n_q}}{A_{n_q}} (-1) \left[\left(\frac{e^{jk|\vec{r}_p - \vec{r}'_q|}}{|\vec{r}_p - \vec{r}'_q|} \right)_{z' \to f_1(x')} - \left(\frac{e^{jk|\vec{r}_p - \vec{r}'_q|}}{|\vec{r}_p - \vec{r}'_q|} \right)_{z' \to f_2(x')} \right] dx' \quad (20)$$

In (20), $f_1(x')$ and $f_2(x')$ are defined as follows:

$$f_1(x') = z'_2 + \left(\frac{z'_2 - z'_3}{x'_2 - x'_3} \right) (x' - x'_2) \quad (21)$$

$$f_2(x') = z'_1 = z'_3 \quad (22)$$

For the second triangle type shown in Fig. 2(b), the analytical evaluation for the integral with the $\frac{\partial}{\partial x'}$ operator is performed as follows:

$$\int_{T_{n_q}} \frac{l_{n_q}}{A_{n_q}} \frac{\partial}{\partial x'} \left(\frac{e^{jk|\vec{r}_p - \vec{r}'_q|}}{|\vec{r}_p - \vec{r}'_q|} \right) ds' = \int_{z'_2}^{z'_1} \int_{f_2(z')}^{f_1(z')} \frac{l_{n_q}}{A_{n_q}} (-1) \frac{\partial}{\partial x'} \left(\frac{e^{jk|\vec{r}_p - \vec{r}'_q|}}{|\vec{r}_p - \vec{r}'_q|} \right) dx' dz'$$

$$= \int_{z'_2}^{z'_1} \frac{l_{n_q}}{A_{n_q}} (-1) \left[\left(\frac{e^{jk|\vec{r}_p - \vec{r}'_q|}}{|\vec{r}_p - \vec{r}'_q|} \right)_{x' \to f_1(z')} - \left(\frac{e^{jk|\vec{r}_p - \vec{r}'_q|}}{|\vec{r}_p - \vec{r}'_q|} \right)_{x' \to f_2(z')} \right] dz' \quad (23)$$

In (23), $f_1(z')$ and $f_2(z')$ are defined as follows:

$$f_1(z') = x'_2 = x'_3 \quad (24)$$

$$f_2(z') = x'_1 + \left(\frac{x'_1 - x'_2}{z'_1 - z'_2} \right) (z' - z'_1) \quad (25)$$

For the same triangle, the analytical evaluation for the integral with the $\frac{\partial}{\partial z'}$ operator is outlined as follows:

$$\int_{T_{n_q}} \frac{l_{n_q}}{A_{n_q}} \frac{\partial}{\partial z'} \left(\frac{e^{jk|\vec{r}_p - \vec{r}'_q|}}{|\vec{r}_p - \vec{r}'_q|} \right) ds' = \int_{x'_1}^{x'_2} \int_{f_2(x')}^{f_1(x')} \frac{l_{n_q}}{A_{n_q}} (-1) \frac{\partial}{\partial z'} \left(\frac{e^{jk|\vec{r}_p - \vec{r}'_q|}}{|\vec{r}_p - \vec{r}'_q|} \right) dz' dx'$$

$$= \int_{x'_1}^{x'_2} \frac{l_{n_q}}{A_{n_q}} (-1) \left[\left(\frac{e^{jk|\vec{r}_p - \vec{r}'_q|}}{|\vec{r}_p - \vec{r}'_q|} \right)_{z' \to f_2(x')} - \left(\frac{e^{jk|\vec{r}_p - \vec{r}'_q|}}{|\vec{r}_p - \vec{r}'_q|} \right)_{z' \to f_1(x')} \right] dx' \quad (26)$$

In (26), $f_1(x')$ and $f_2(x')$ are defined as follows:

$$f_1(x') = z'_1 = z'_3 \quad (27)$$

$$f_2(x') = z'_1 + \left(\frac{z'_1 - z'_2}{x'_1 - x'_2} \right) (x' - x'_1) \quad (28)$$

After the analytical treatment, the integrals in (17), (20), (23) and (26) are computed using a 80 point Gaussian quadrature rule given in [2].

The matrix equation in (2) is solved using the least squares QR(LSQR) method [3]. The LSQR method is a preferred iterative method for the solution of highly ill-conditioned systems [4]. The LSQR solution is carried out in Fortran90 by adapting the module named "zlsqrmodule.f90" [5]. The Fortran90 codes are compiled by the GNU Fortran compiler gfortran-4.7.

3. RESULTS

The integrals in (15) are first computed fully numerically using a 79 point Gaussian quadrature rule for the triangle given in [6]. Then, they are computed using the semi-analytical method. The source reconstruction is performed for both of the fully numerical and semi-analytical solution schemes. The programs written for the solution of the source reconstruction problem are in Fortran90 language. The compiler is the GNU Fortran compiler gfortran-4.7. The matrix vector products have been carried out using automatically tuned linear algebra software (ATLAS) with a linear algebra package (LAPACK). The operation frequency is 1 GHz. The medium is the free space. The source reconstruction plane is a square of side 0.3 m. The original source is at the center of the square. The square is meshed using NX 9.0 with a mesh side of $\lambda/\sqrt{300}$. The electric field data is obtained on the surface of a hemisphere with radius of 1 m and center coinciding with the center of the square. The current reconstruction is made at centroids of the mesh elements which are triangles shown in Fig. 2.

In Fig. 3, the magnitudes of the x and z components of the current density reconstructed by means of the fully numerical procedure are shown. It can be observed that the x component of the source tends to concentrate at the center of the source reconstruction plane. The average magnitude of the z component is small compared to that of the x component. This result is expected since the original source has only an x component.

In Fig. 4, the magnitudes of the x and z components of the current density reconstructed by means of the semi-analytical procedure are displayed. A behavior similar to the results of the fully

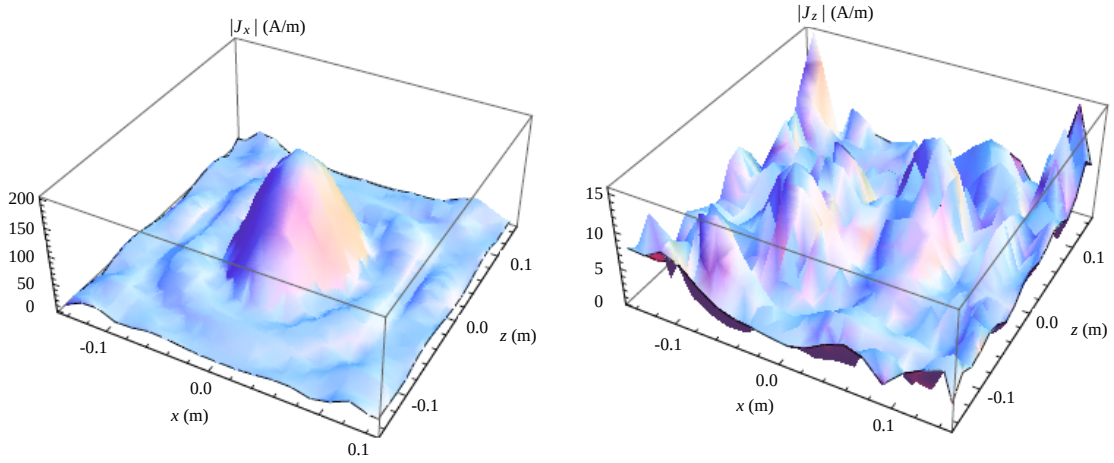

Figure 3. The reconstructed current magnitudes for the fully numerical procedure.

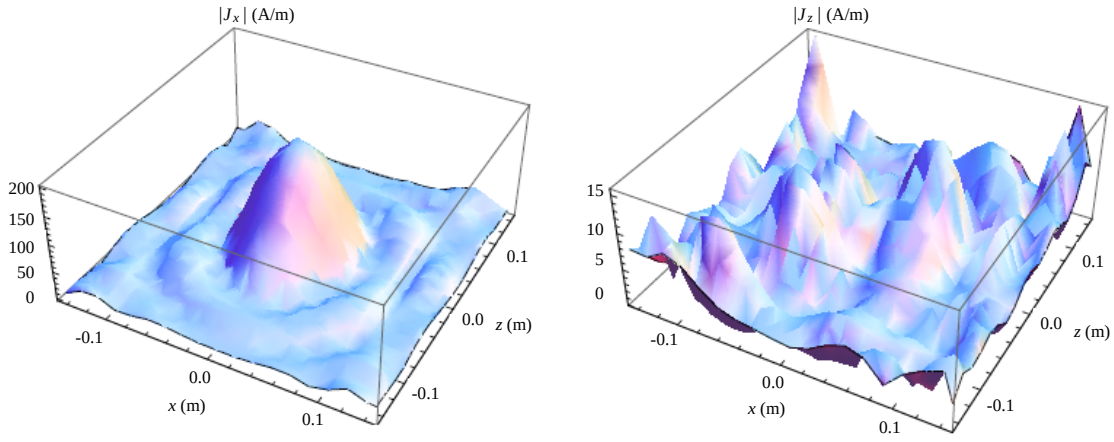

Figure 4. The reconstructed current magnitudes for the semi-analytical procedure.

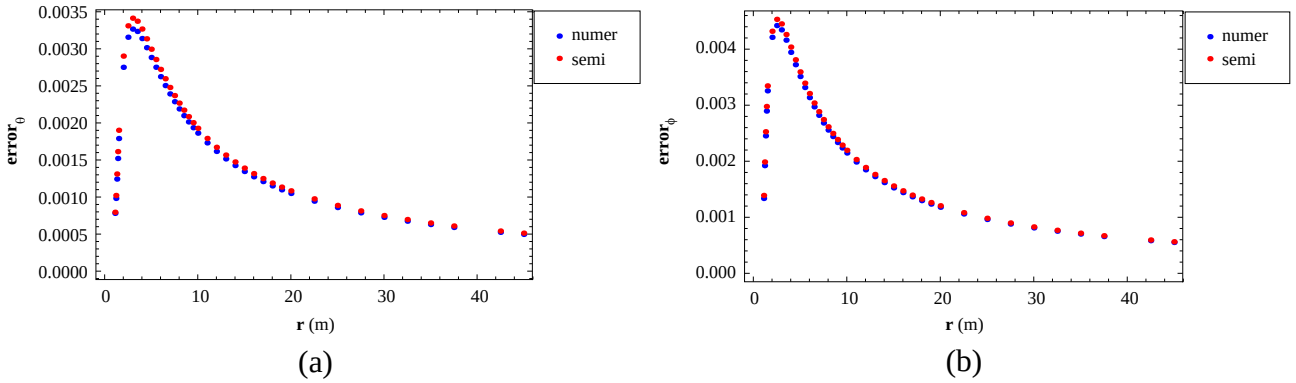

Figure 5. The plots of the error in the reconstructed field components for the fully numerical and the semi-analytical procedures. (a) The error in reconstructed E_θ. (b) The error in reconstructed E_ϕ.

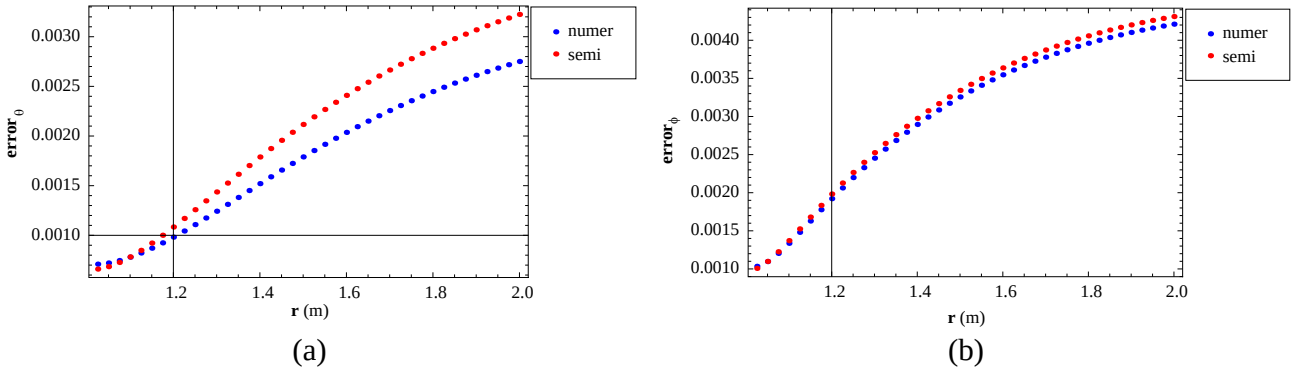

Figure 6. The plots of the error in the reconstructed near field components for the fully numerical and the semi-analytical procedures. (a) The error in the reconstructed near E_θ. (a) The error in the reconstructed near E_ϕ.

numerical procedure is observed in these results. Hence, the semi-analytical procedure works well in the reconstruction of the original source.

As a further verification, the electric field of the reconstructed current is calculated as a function of the distance and compared to the field due to the original source. The error made is defined as follows:

$$\text{error} = \sqrt{\frac{\sum_{i=1}^{M} |computed_i - actual_i|^2}{M}} \tag{29}$$

where $computed_i$ is the ith element of the computed field vector and $actual_i$ is the ith element of the actual field vector. M is the number of field sampling points. In Fig. 5, the error made in the reconstructed electric field components are displayed for the fully numerical procedure and the semi-analytical procedure. It is observed that the errors are close to each other. Hence, it is again verified that the semi-analytical procedure performs well. In Fig. 6, for a better comparison for the near field prediction, the plot of the error in the reconstructed field components are drawn versus the radius of the reconstruction surface as r is increased from 1.25 m to 2 m with an increment of 0.025 m. From the Fig. 6, it can observed that the semi-analytical approach performs well in the prediction of the very near field as well.

4. CONCLUSION

In this article, a simple semi-analytical method is proposed to calculate the entries of the moments matrix obtained by the discretization of a mixed potential integral equation. The semi-analytical method is shown to work well. The method makes use of a differentiation property of the scalar Green's function and the structure of the mesh elements forming the source reconstruction plane. Since the method enables a partial analytical calculation in the integrals of the moments matrix entries, the accuracy of the moments matrix elements can be increased more easily using the semi-analytical method. The method is applicable to any integral equation solved using the method of moments with point matching.

ACKNOWLEDGMENT

The software NX 9.0 used for meshing has been granted by Siemens. The author has been acquainted with the source reconstruction and LSQR method during a short visit to Bilkent University Computational Electromagnetics Center (BİLCEM) and would like to thank Prof. Levent Gürel and the staff of BİLCEM.

REFERENCES

1. Rao, S. M., D. R. Wilton, and A. W. Glisson, "Electromagnetic scattering by surfaces of arbitrary shape," *IEEE Trans. Antennas Propag.*, Vol. 30, No. 3, 409–428, 1982.
2. Abramowitz, M. and I. A. Stegun, *Handbook of Mathematical Functions with Formulas, Graphs, and Mathematical Tables*, US Government Printing Office, 1965.
3. Paige, C. C. and M. A. Saunders, "LSQR: An algorithm for sparse linear equations and sparse least squares," *ACM Transactions on Mathematical Software*, Vol. 8, No. 1, 43–71, Mar. 1982.
4. Hansen, P. C., *Rank-deficient and Discrete Ill-posed Problems: Numerical Aspects of Linear Inversion*, SIAM, 1997.
5. Saunders, M. A., "zlsqrmodule.f90," Jun. 29, 2013, Online Available: http://web.stanford.edu/group/SOL/software/lsqr/f90/zlsqr.zip.
6. Dunavant, D. A., "High degree efficient symmetrical gaussian quadrature rules for the triangle," *International Journal for Numerical Methods in Engineering*, Vol. 21, 1129–1148, 1985.
7. Petre, P. and T. K. Sarkar, "Planar near-field to far-field transformation using an equivalent magnetic current approach," *IEEE Trans. Antennas Propag.*, Vol. 40, No. 11, 1348–1356, Nov. 1992.
8. Taaghol, A. and T. K. Sarkar, "Near-field to near/far-field transformation for arbitrary near-field geometry, utilizing an equivalent magnetic current," *IEEE Trans. Electromagn. Compat.*, Vol. 38, No. 3, 536–542, Aug. 1996.
9. Sarkar T. K. and A. Taaghol, "Near-field to near/far-field transformation for arbitrary near-field geometry, utilizing an equivalent electric current and MOM," *IEEE Trans. Antennas Propag.*, Vol. 47, No. 3, 566–573, Mar. 1999.
10. Las-Heras, F., B. Galocha, and J. L. Besada, "Far-field performance of linear antennas determined from near-field data," *IEEE Trans. Antennas Propag.*, Vol. 50, No. 3, 408–410, Mar. 2002.
11. Las-Heras, F. and T. K. Sarkar, "A direct optimization approach for source reconstruction and NF-FF transformation using amplitude-only data," *IEEE Trans. Antennas Propag.*, Vol. 50, No. 4, 500–510, Apr. 2002.
12. Las-Heras, F. and T. K. Sarkar, "Radial field retrieval in spherical scanning for current reconstruction and NF-FF transformation," *IEEE Trans. Antennas Propag.*, Vol. 50, No. 6, 866–874, Jun. 2002.
13. Alvarez, Y., F. Las-Heras, and M. R. Pino, "Reconstruction of equivalent currents distribution over arbitrary three-dimensional surfaces based on integral equation algorithms," *IEEE Trans. Antennas Propag.*, Vol. 55, No. 12, 3460–3468, Dec. 2007.
14. Alvarez, Y., F. Las-Heras, and M. R. Pino, "Probe-distortion correction for the sources reconstruction method," *IEEE Antennas and Propagation Mag.*, Vol. 50, No. 6, 117–124, Dec. 2008.

15. Arrebola, M., Y. Alvarez, J. A. Encinar, and F. Las-Heras, "Accurate analysis of printed reflectarrays considering the near field of the primary feed," *IET Microw. Antennas Propag.*, Vol. 3, No. 2, 187–194, 2009.
16. Eibert, T. F. and C. H. Schmidt, "Multilevel fast multipole accelerated inverse equivalent current method employing Rao-Wilton-Glisson discretization of electric and magnetic surface currents," *IEEE Trans. Antennas Propag.*, Vol. 57, No. 4, 1178–1185, Apr. 2009.
17. Lopez, Y. A., F. Las-Heras, M. R. Pino, and T. K. Sarkar, "An improved super-resolution source reconstruction method," *IEEE Trans. Instrum. Meas.*, Vol. 58, No. 11, 3855–3866, Nov. 2009,
18. Persson, K., M. Gustafsson, and G. Kristensson, "Reconstruction and visualization of equivalent currents on a radome using an integral representation formulation," *Progress In Electromagnetics Research B*, Vol. 20, 65–90, 2010.
19. Lopez, Y. A., A. Dominguez-Casas, C. Garcia-Gonzalez, and F. Las-Heras, "Geometry reconstruction of metallic bodies using the sources reconstruction method," *IEEE Trans. Propag. Lett.*, Vol. 9, 1197–1200, Dec. 2010.
20. Alvarez, Y., M. Rodriguez, F. Las-Heras, and M. M. Hernando, "On the use of the source reconstruction method for estimating radiated EMI in electronic circuits," *IEEE Trans. Instrum. Meas.*, Vol. 59, No. 12, 3174–3183, Dec. 2010.
21. Lopez-Fernandez, J. A., M. Lopez-Portugues, Y. Alvarez-Lopez, C. Garcia-Gonzalez, D. Martinez, and F. Las Heras Andres, "Fast antenna characterization using the sources reconstruction method on graphics processors," *Progress In Electromagnetics Research*, Vol. 126, 185–201, 2012.
22. Vazquez, C., C. Garcia, Y. Alvarez, V. Ver-Hoeye, and F. Las-Heras, "Near field characterization of an imaging system based on a frequency scanning antenna array," *IEEE Trans. Antennas Propag.*, Vol. 61, No. 5, 2874–2879, May 2013.
23. Li, P., Y. Li, L. J. Jiang, and J. Hu, "A wide-band equivalent source reconstruction method exploiting the Stoer-Bulirsch algorithm with the adaptive frequency sampling," *IEEE Trans. Antennas Propag.*, Vol. 61, No. 10, 5338–5343, Oct. 2013.
24. Li, P. and L. J. Jiang, "An iterative source reconstruction method exploiting phaseless electric field data," *Progress In Electromagnetics Research*, Vol. 134, 419–435, 2013.
25. Lopez-Portugues, M., Y. Alvarez, J. A. Lopez-Fernandez, C. Garcia-Gonzalez, R. G. Ayestaran, and F. Las Heras Andres, "A multi-GPU sources reconstruction method for imaging applications," *Progress In Electromagnetics Research*, Vol. 136, 703–724, 2013.
26. Quijano, J. L. A. and G. Vecchi, "Improved-accuracy source reconstruction on arbitrary 3-D surfaces," *IEEE Trans. Propag. Lett.*, Vol. 8, 1046–1049, Sep. 2009.
27. Quijano, J. L. A. and G. Vecchi, "Near- and very near-field accuracy in 3-D source reconstruction," *IEEE Trans. Propag. Lett.*, Vol. 9, 634–637, Sep. 2010.
28. Quijano, J. L. A. and G. Vecchi, "Field and source equivalence in source reconstruction on 3D surfaces," *Progress In Electromagnetics Research*, Vol. 103, 67–100, 2010.
29. Quijano, J. L. A., L. Scialacqua, J. Zackrisson, L. J. Foged, M. Sabbadini, and G. Vecchi, "Suppression of undesired radiated fields based on equivalent currents reconstruction from measured data," *IEEE Trans. Propag. Lett.*, Vol. 10, 314–317, Apr. 2011.
30. Foged, L. J., L. Scialacqua, F. Saccardi, J. L. A. Quijano, and G. Vecchi, "Application of the dual-equation equivalent-current reconstruction to electrically large structures by fast multipole method enhancement," *IEEE Antennas and Propagation Mag.*, Vol. 56, No. 5, 264–273, Oct. 2014.